

# Gear and bearing fault detection under variable operating conditions

Pavle Boškosi<sup>1</sup>, Đani Juričić<sup>1</sup>, and Mile Stankovski<sup>2</sup>

<sup>1</sup> *Jožef Stefan Institute, Jamova cesta 39, 1000 Ljubljana, Slovenia*  
pavle.boskoski@ijs.si  
dani.juricic@ijs.si

<sup>2</sup> *Faculty of Electrical Engineering and Information Technologies*  
*University Ss. Cyril and Methodius, 1000 Skopje, Macedonia*  
milestk@feit.ukim.edu.mk

## ABSTRACT

The majority of the approaches to the fault detection in rotational machines assume constant and known operating conditions. These assumptions are often violated in practice. Therefore, in this paper we propose a set of features that can be utilized to reveal faults in gearboxes while being robust to fluctuations in operating speed and load. The proposed feature set comprises values of two information cost functions calculated from the coefficients of the wavelet packet transform accompanied by the maximal value of the spectral kurtosis. The fault detection capabilities of the proposed feature set were evaluated on a two-stage gearbox operating under different rotational speeds and loads with different types of mechanical faults.

## 1. INTRODUCTION

The traditional vibration based fault detection approaches rely on the assumption that the changes in the features' values are directly related with the changes in the condition of the monitored machine. This assumption, provided the monitored machine operates under constant load and constant rotational speed, is valid since any fluctuations in the operating conditions might affect either the amplitude or the frequency signatures of the vibrational patterns. Therefore, under variable operating conditions the deterioration in the machine health can not be unambiguously addressed as the unique cause for the observed changes in the feature values. The idea of this paper is to investigate a set of features that react to the faults in mechanical drives while being robust to the changes in operating conditions.

The problem of fault detection under fluctuating load and speed has received commendable attention in the area of rotational machines. Most of the proposed solutions employ information about the current operating condition in order to properly handle the underlying feature values. In that manner, fault detection under vari-

able operating speed is usually performed by applying time-synchronous average (TSA) (Zhan, Makis, & Jardine, 2006). Similarly, information about the instantaneous speed is often used in the process of monitoring gears subjected to fluctuating conditions (Stander & Heyns, 2005). There are examples of using higher order spectra analysis for the detection of various bearing faults under different load conditions (Parker et al., 2000). Taking into account the information about both variations in speed and load, a specific feature set was defined by Bartelmus and Zimroz for fault detection in multi-stage gearboxes (Bartelmus & Zimroz, 2009). Although the proposed approaches give satisfactory results they heavily depend on accurate measurements of the current speed and load of the monitored gearbox.

Need for precise information about current operating conditions can be evaded by exploiting the specific structure of the vibrational patterns produced by bearings' and gears' surface faults. These faults are characterized by specific amplitude modulations in the vibrations as well as by the occurrence of broad-band spectral components. By observing how these artifacts influence the statistical behavior of the vibration signals in time and in frequency domain we can extract a specific set of features that can be used to characterize the current machine state without precise knowledge of the operating conditions.

In the process of estimating the statistical characteristics of the underlying vibrations, one has to consider the fact that vibrations produced by a rotational machine under varying operating conditions are in essence non-stationary signals. One of the main pillars in the analysis of such signals is the concept of evolutionary spectra (Priestley & Gabr, 1993), i.e. the evolution of the power spectrum in time. Based on this concept Baydar and Ball have performed detection of gear deterioration under different loads using instantaneous power spectrum by employing Wigner-Ville distribution (WVD) (Baydar & Ball, 2000). However, the proposed approach is computationally expensive and the analysis requires visual inspection of the WVD maps.

These problems can be overcome by the application of the wavelet transform as a tool for analysis of non-stationary signals (Spanos & Failla, 2004). The analy-

This is an open-access article distributed under the terms of the Creative Commons Attribution 3.0 United States License, which permits unrestricted use, distribution, and reproduction in any medium, provided the original author and source are credited.

sis of non-stationary signals using wavelet transform has proved to be effective in the field of neuroscience for the analysis of brainwave signals (Rosso et al., 2001). Based on the wavelet coefficients one can calculate the so called information cost functions (ICFs) that can be associated with the distribution of the signal's energy in both time and frequency domain. These functions have basic form of an entropy-like function, thus they give an estimation about the disorder in the system (Figliola & Serrano, 1997). Based on the features extracted from such entropy-like functions Feng and Schlindwein have devised a fault detection system for surface bearing faults (Feng & Schlindwein, 2009). They have shown that both fault detection and fault isolation of different bearing faults can be successfully conducted by applying features extracted from the ICFs. In our approach we extend this concept by calculating the ICFs for the vibration signals produced by two-stage gearbox running under different operating conditions with different kind of gear and bearing faults. For the sake of better diagnostic resolution, the feature set was enriched by adding an additional feature defined as a maximal value of the spectral kurtosis (SK) (Antoni & Randall, 2006). The obtained feature set was afterwards used to perform the fault detection task. The obtained results support the hypothesis that a faulty case can be distinguished from the fault-free case just by observing the values of the ICFs and the maximal value of SK, without any knowledge of the current operating conditions.

The paper is organized in the following manner. A brief overview of the specific vibrational patterns produced by gears and bearings is presented in Section 2.. The concepts behind the calculation of the ICFs and SK are given in Section 3.. Finally, in Section 4. we will present the results of the fault detection performed using the defined feature set.

## 2. MECHANICAL FAULTS SIGNATURES

Accurate fault detection of a running gearbox depends on the ability of inferring about the state of each mechanical element only by observing the produced vibrations. These vibrations comprise the vibrations produced by each rotating element together with their mutual interactions. Therefore, it is crucial to be able to distinguish the changes in the vibrational patterns emanated from a particular element.

### 2.1 Vibrations produced by running gears

The vibrations produced by a healthy gearbox are dominated by the vibration components produced by meshing gears. In the cases of spur gears, these vibrations are product of the mesh stiffness variation that occurs as the number of teeth in contact oscillates between one and two teeth (Howard, Jia, & Wang, 2001). Consequently the resulting vibrations are characterized by prominent spectral components located at the harmonics of mesh frequency (Kuang & Li, 2003). Additionally, these components are accompanied by modulation components originating from the assembly errors and the fluctuation in the gears speed and load. Thus, the vibrations  $x(t)$  produced by a meshing gears can be written as

follows (Wang, 2001):

$$x(t) = \sum_{m=0}^M A_m (1 + a_m(t)) \cos(2\pi f_m t + \beta_m + b_m(t)), \quad (1)$$

where  $m$  is the meshing harmonic,  $A_m$  and  $f_m$  the amplitude and the frequency of the  $m^{th}$  harmonic of the gear mesh frequency respectively. The components  $a_m(t)$  and  $b_m(t)$  are the amplitude and phase modulations respectively, and  $\beta_m$  is the initial phase. It should be noted that the amplitudes  $A_m$  depend on the applied load on the gears.

In cases of localized faults the vibration model (1) should be expanded in order to accommodate the impacts occurring in damaged areas. These impacts, over a course of one revolution, can be modeled as:

$$z(t) = d(t) \cos(2\pi f_r t + \theta_r), \quad (2)$$

where  $d(t)$  is the envelope marking the impact moments that excite resonant oscillations with frequency  $f_r$  and phase  $\theta_r$ .

### 2.2 Vibrations produced by localized bearing faults

Unlike gears, healthy bearings produce no or negligible vibrations. However in case of bearing's surface damage they produce a vibrational patterns similar to the impacts (2) produced by the damaged gears. These vibrations are generated by the bearing balls passing through the damaged surface. Each time this happens the impact between the passing ball and the damaged surface excites the system's impulse response  $s(t)$ . Under constant operating conditions these impacts may be approximated as truly periodic, with a period directly connected to the type and the location of the surface fault. However, under variable operating conditions the occurrence of these impacts should be treated as purely random events. Furthermore, the amplitude of each impulse response also differs, due to changes in the surfaces and the microscopic variation how each roller element enters the load zone. These fluctuations in the amplitudes and period of occurrence of impulse response were modeled by Randall, Antoni, and Chobsaard (Randall et al., 2001) as:

$$x(t) = \sum_{i=-\infty}^{+\infty} A_i s(t - \tau_i) + n(t), \quad (3)$$

where  $A_i$  is the random amplitude of the  $i^{th}$  impulse response,  $\tau_i$  is the time its occurrence. The final component,  $n(t)$ , defines an additive random component that contains all non-modeled vibrations as well as environmental disturbances.

## 3. OVERVIEW OF THE SIGNAL PROCESSING METHODS

Regarding the both conceptual models, presented in Section 2., the vibrations produced by a healthy gearbox are dominated by strong components at the gear mesh frequency and its sidebands. Despite the possible fluctuations in the operating conditions, in short term the produced vibrations can be characterized by a specific time varying patters which are result from the modulation generated by the meshing gears. The occurrence of

a fault causes two significant changes in the overall vibrational signal: occurrence of new modulation and appearance of new spectral components as a result of the excitation of additional eigenmodes. Therefore, the effectiveness of the fault detection process lies in the ability to detect these changes.

In cases of constant operating conditions, the analysis of the vibration signals is usually performed under assumption that signals are stationary, at least in a given time window. However, under variable operating conditions this assumption is invalid and the signals have to be treated as non-stationary. Consequently, the analysis of the signals was performed using two signal processing techniques suitable for non-stationary signal analysis: wavelet transform and spectral kurtosis.

### 3.1 Wavelet analysis

The wavelet analysis is based on a smooth and quickly vanishing oscillating functions called the wavelets. Such functions offer good localization in both time and frequency domain. Typically the wavelet transform is based on a family of wavelets created by dilatation  $s$  and translation  $u$  of a mother wavelet  $\psi_{u,s}(t)$  (Mallat, 1999):

$$\psi_{u,s}(t) = \frac{1}{\sqrt{s}} \psi\left(\frac{t-u}{s}\right) \quad (4)$$

Consequently the wavelet transform of a function  $f(t)$  is defined as:

$$Wf(s, u) = \int_{-\infty}^{+\infty} f(t) \frac{1}{\sqrt{s}} \psi^*\left(\frac{t-u}{s}\right) dt, \quad (5)$$

where  $\psi^*(t)$  represents the complex conjugate of the underlying wavelet function.

Calculation of the wavelet transform (5) can be limited to a set of discrete values for the parameters  $s$  and  $u$ , namely  $s_j = 2^{-j}$  and  $u_{j,k} = 2^{-j}k$ , where  $j, k \in \mathbb{Z}$ . Hence the mother wavelet (4) becomes:

$$\psi_{j,k}(t) = 2^{j/2} \psi(2^j t - k), \quad j, k \in \mathbb{Z}. \quad (6)$$

The wavelet transform (5) with the restriction (6) is referred to as discrete wavelet transform (DWT) (Figliola & Serrano, 1997). The wavelet coefficients  $c_{j,k}$  can be calculated using the inner product

$$c_{j,k} = Wf(s_j, u_{j,k}) = \langle f(t), \psi_{j,k}(t) \rangle. \quad (7)$$

Finally a given function  $f(t)$  can be decomposed using DWT as

$$f(t) = \sum_j \sum_k c_{j,k} \psi_{j,k}(t). \quad (8)$$

The classical DWT results in a logarithmic frequency resolution (Burrus, Gopinath, & Guo, 1994). An upgrade to this approach is the finer adjustment of the frequency resolution for both high and low frequency bands. This results into the so called wavelet packet transform (WPT) in which the selection of the time-frequency resolution can be adjusted in both high and low frequencies. Consequently, WPT produces a wavelet packet tree with depth  $D_0$  with nodes  $(d, n)$ , where  $d = \{1, \dots, D_0\}$  represents the depth of the tree, and  $n = 0, \dots, 2^d - 1$  represents the number of the node at depth  $d$  (cf. Figure 1). Each of the  $n$  nodes at level  $d$  contains  $N_d$  wavelet coefficients  $\mathbf{W}_{d,n,t}$ ,  $t = 0, \dots, N_d - 1$  (Percival & Walden, 2000).

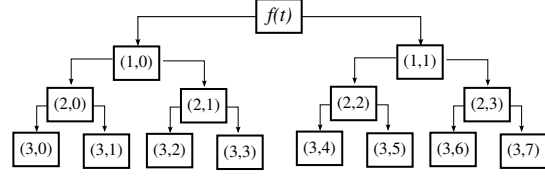


Figure 1: Structure of WPT tree with depth  $D_0 = 3$

### Information cost functions

Wavelet transforms including WPT is performed using family of wavelets  $\psi_{j,k}(t)$  that build orthonormal basis. Under such condition the energy of the original signal  $f(t)$  is related to the wavelet coefficients (7), similarly like in the case of Fourier transform. Consequently, the wavelet transform enables localization of the signal's energy in both time and frequency with resolution guided by the uncertainty principle. For the case of WPT the signal's energy can be obtained only by observing the coefficients in the terminal nodes (Blanco, Figliola, Quiroga, Rosso, & Serrano, 1998):

$$E_{tot} = \sum_{\substack{t=0 \\ d,n \in C_t}}^{N_d-1} \|\mathbf{W}_{d,n,t}\|^2, \quad (9)$$

where  $C_t$  represents the set of terminal nodes. Equivalently, the energy contained within one node  $(d, n)$  can be calculated as:

$$E_{d,n} = \sum_{t=0}^{N_d-1} \|\mathbf{W}_{d,n,t}\|^2 \quad (10)$$

Using the equations (9) and (10) we can obtain the distribution of the signal's energy over the terminal nodes  $C_t$  as follows:

$$p_{d,n}(f) = \frac{E_{d,n}}{E_{tot}} \quad (11)$$

Since each terminal node covers a specific frequency interval the relation (11) in essence gives the signal's energy distribution over frequency.

Similarly we can define the distribution of the signal's energy in time. This distribution can be given for each node  $(d, n)$  as:

$$p_{d,n}(t) = \frac{|\mathbf{W}_{d,n,t}|^2}{E_{d,n}}, \quad t = 0, \dots, N_d - 1, \quad (12)$$

where  $E_{d,n}$  is the energy contained within the  $(d, n)$  node, as defined with (10).

Based on these two distributions the entropy-like Information Cost Functions (ICFs) can be defined as (Rosso et al., 2001; Zunino, Pérez, Garavaglia, & Rosso, 2007):

$$C_t = - \sum_{t=0}^{N_d-1} p_{d,n}(t) \log_2(p_{d,n}(t)), \quad (13)$$

and

$$C_f = - \sum_{d,n \in C_t} p_{d,n}(f) \log_2(p_{d,n}(f)). \quad (14)$$

The first function (13) shows whether time waveform exhibits some repetitive pattern. In such a case, the wavelet pattern in the specific node  $(d, n)$  will correspond to the repetitive signal's pattern. Therefore, the corresponding wavelet coefficients  $W_{d,n,t}$  will acquire high value, according to (7), where as all the other wavelet coefficients will have significantly lower values. Consequently, the entropy-like function (13) will acquire very low value. Conversely, if the corresponding signal shows erratic or random behavior none of the wavelet coefficients will have high value since every signal part will significantly differ from the used wavelet function. Consequently, most of the coefficients will have similar values hence  $C_t$  will acquire high value.

The second function (14), on the other hand, can be employed to describe the signals frequency signature. If the observed signal is narrow-band, the majority of the energy will be concentrated within a limited number of terminal nodes. However, if the signal exhibits broad-band components the energy will be spread over several terminal nodes, which consequently will lead to the higher values for  $C_f$ .

### 3.2 Spectral kurtosis

The spectral kurtosis (SK) was firstly introduced by Dwyer, as a method that is able to distinguish between transients (impulses and unsteady harmonic components) and stationary sinusoidal signals in background Gaussian noise (Dwyer, 1983). The method was introduced in the field of fault detection by Antoni and Randall, and has proved effective in detecting faults in gears and bearings (Antoni & Randall, 2006).

The underlying value gives an estimate of the fraction of the overall signal energy caused by strong and sporadic impulses relative to the energy of mild and frequent oscillations. Applying this concept to the amplitudes of the signal's spectral components, we obtain information about the frequency band in which such sudden bursts of energy are mostly expressed. Considering that both surface gear (2) and bearing faults (3) are characterized by a sporadic excitations of system's eigenmodes, the SK method turns to be a suitable approach for the detection of these excitations.

The value of SK can be roughly estimated from the short-time Fourier transform (STFT). Applying STFT with an arbitrary window to a non-stationary signal we obtain a series of amplitude spectra  $S(t, f)$  for each time position of the chosen window. The standard power spectral density can be obtained as a time average of these spectra. The spectral kurtosis on the other hand is obtained by calculating the fourth order moment of these complex spectra:

$$SK(f) = \frac{\langle S(t, f)^4 \rangle}{\langle S(t, f)^2 \rangle^2} - 2. \quad (15)$$

The equation (15) differs from the standard relation for kurtosis in the subtraction factor, which in this case is 2 instead of the standard 3. This change is due to the fact that the spectra  $S(f, t)$  can be treated as a complex random variables that have circular nature.

## 4. RESULTS

### 4.1 Experimental runs

The experimental data was acquired on a laboratory two-stage gearbox (PHM, 2009) (cf. Figure 2). The test runs include 7 different fault combinations and one fault-free reference run. Each set-up was tested under 5 different rotational speeds of the input shaft: 30, 35, 40, 45 and 50 Hz. Additionally two different load levels were applied. Furthermore, each combination of different fault, speed and load was measured in two different measurements. As a result of this configuration we have 160 different measurements.

The detailed list of the introduced faults is listed in Table 1. It should be noted that bearing faults were introduced only on the bearings 1–3, and all the remaining bearings were kept fault-free during the whole experimental runs. Additionally, the shaft imbalance was introduced on the *Input shaft*, whereas the sheared keyway fault was located on the *Output shaft*.

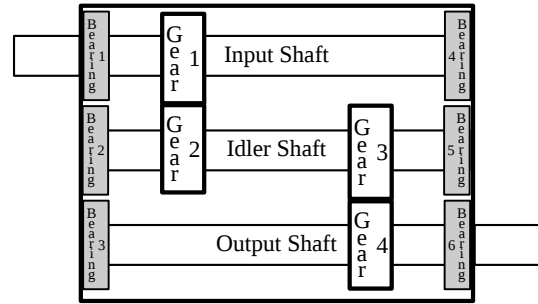


Figure 2: Schematic description of the used two-stage gearbox

### 4.2 Evaluation of the feature set

In the presence of mechanical faults, two major changes occur in vibrations produced by the observed gearbox:

- the appearance of new patterns in the signal's time waveform, and
- the changes in the energy distribution over the observed frequency range.

These changes can be detected from variations of the value of SK and the values of the wavelet packet's ICFs.

**Spectral Kurtosis** For the purpose of fault detection we have calculated SK for each experimental run. The distributions of the maximal SK values for each experimental run, for both load levels are shown in Figure 3.

By comparing the SK values for the experimental runs under low and high load, shown in Figures 3a and 3b respectively, we can observe the following:

1. The SK for the fault-free run (#1) in both cases has median value around 9.5 and small interquartile dispersion. Therefore, we can regard this value to be invariant to the changes of the speed and load;
2. The experimental runs #4, #6–8 have significantly higher value for SK than the fault-free run regardless of the operating conditions;

Table 1: Fault details for each experimental run

Run Number	Gear				Bearing <sup>1</sup>			Shaft fault
	1	2	3	4	1	2	3	
#1	Fault Free (FF)							
#2	Chipped	FF	Eccentric	FF	Fault Free (FF)			
#3	FF	FF	Eccentric	FF	Fault Free (FF)			
#4	FF	FF	Eccentric	Broken	Inner	Ball	FF	FF
#5	Chipped	FF	Eccentric	Broken	Inner	Ball	Outer	FF
#6	FF	FF	FF	Broken	Inner	Ball	Outer	Imbalance
#7	FF	FF	FF	FF	Inner	FF	FF	Keyway Sheared
#8	FF	FF	FF	FF	FF	Ball	Outer	Imbalance

<sup>1</sup> Faults were introduced only on Bearings 1–3 (cf. Figure 2). The other three bearings were kept fault-free during all experimental runs.

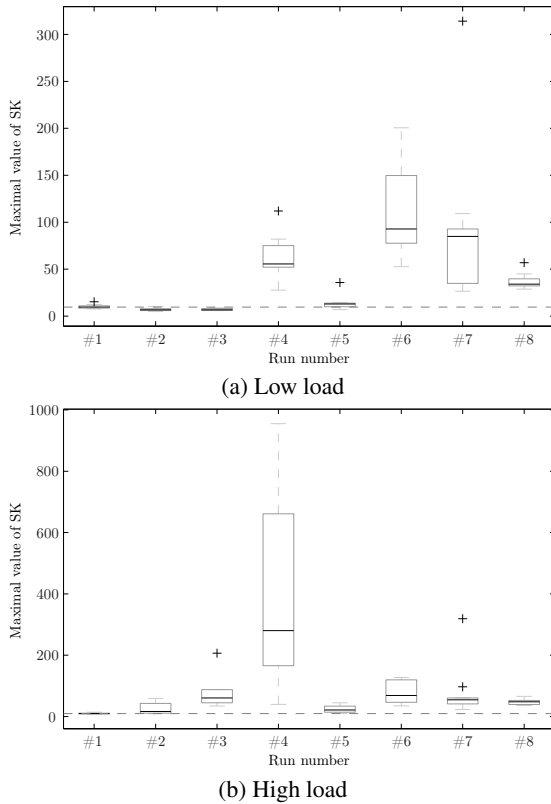


Figure 3: Spread of the maximal spectral kurtosis value for each experimental run over different speeds

- The experimental run #5 in both cases has values near the fault-free run. In particular, the median of the SK for low load is 13 and for the high load is 21; and
- Finally the experimental runs #2 and #3 show significant variation between the low load and high load runs. In case of high load the SK value is higher than the fault-free run and in the low-load it is lower than the fault-free run.

The high values of SK for experimental runs #4, #6–8 can be attributed to the bearing's surface damages. According to the bearing vibration model (3) vibrations of the damaged bearings are rich with randomly occurring

impulses. As a result of this effect, the underlying experimental runs exhibit significantly higher SK values than the fault-free run, regardless of the operating conditions.

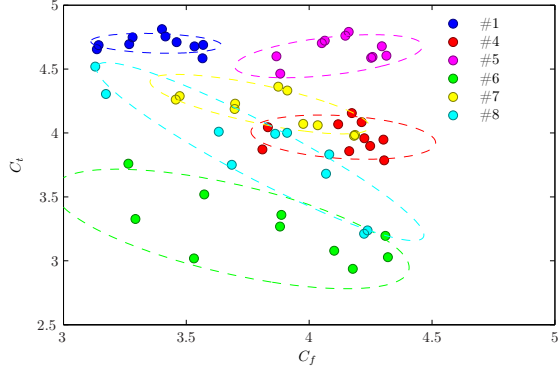
The experimental run #5 includes a combination of a severe gear fault and bearing damage. Despite the presence of the bearing faults, the most dominant source of vibrations can be found in the severe gear damage. However, since the damage of the gears were artificially made only on one gear tooth, the impacts (2) have occurred only once per rotation. As a result of this, the influence of these impacts on the overall signals energy is not so significant. Thus, the value of the SK is lower despite the presence of a bearing fault.

Significant difference in the value of SK between the low and high load runs can be noticed for the experimental runs #2 and #3. The explanation follows from the mechanism behind the gear vibrations. According to the gear vibration model (1) and (2), the amplitude of the produced vibrations for the dominant spectral components  $A_m$  depend on the applied load. As a result of this effect, the SK values significantly differs between the runs conducted under high and low load. Furthermore, the absence of bearing faults removes random impulses that were present in the experimental run #5, which proves to be a crucial difference.

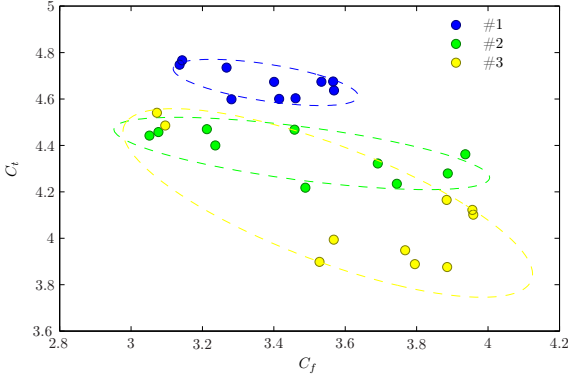
From the performed experimental runs we can conclude that the maximal value of the spectral kurtosis is capable of detecting faults that are characterized by a repetitive impulse bursts. Most commonly, such bursts occur in cases of bearing surface damage. Therefore, the experimental runs containing bearing faults show significant changes in the SK values (#4,6–8).

However, the experimental run #5 is an exception to this observation. Despite the presence of bearing fault the value of SK is similar to the fault-free run. Furthermore, in cases of pure gear faults (#2 and #3) the load level significantly influences the value of SK. Therefore, in order to overcome these shortcomings we have expanded the candidate feature set by adding two more features extracted from the wavelet packet coefficients as described in the next section.

**Wavelet packet ICFs** Both load cases were analyzed using WPT with *db10* mother wavelet. Each experimental run was analyzed using 4-levels WPT tree, which produces 16 terminal leaves. Signals were divided into segments each covering approximately 3 rotations at the lowest speed.



(a) Experimental runs with mixed gear and bearing faults



(b) Experimental runs only with gear faults

Figure 4: Values of the ICFs for the experimental runs conducted under high load. The dashed lines represent the dispersion of the feature values for each experimental run

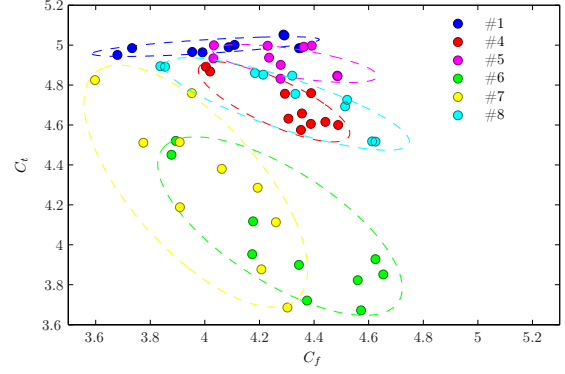
Values of both ICFs (11) and (12) for the high load experimental runs are shown in Figure 4. The values of ICFs from experimental runs with the same faults tend to group into “clusters”. The cluster from the reference fault-free run (#1) is located in the upper left corner of the plots. In respect to the fault-free cluster, clusters from other faults have two distinct characteristics: higher value for  $C_f$  ( $x$ -axis) and lower value for  $C_t$  ( $y$ -axis).

The increase in the value of  $C_f$  is an indicator that vibration spectrum is spread over a broader range of frequencies compared to the fault-free run. This is a consequence of an additionally excited system’s eigenmode which contributes to a “richer” frequency signature.

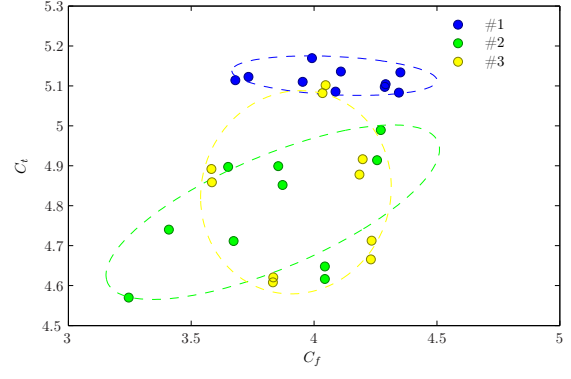
The lower value for  $C_t$  can be treated as an indicator that the signal contains a specific patterns in the time domain that distinguish it from an unordered noise. In cases of the observed mechanical faults these effects are a result of an additional modulation components produced by the underlying fault.

The dispersion of the values of  $C_f$  and  $C_t$  can be analyzed by dividing the results into two segments:

1. dispersion of ICFs for experimental runs containing combined bearing–shaft and gear–bearing faults (cf. Figure 4a); and
2. dispersion of ICFs for cases of the experimental runs conducted only with gear faults (cf. Figure 4b).



(a) Experimental runs with mixed gear and bearing faults



(b) Experimental runs only with gear faults

Figure 5: Values of the ICFs for the experimental runs conducted under low load. The dashed lines represent the dispersion of the feature values for each experimental run

The increase of the  $C_f$  is most evident in the experimental runs that contain bearing faults (#4–8) (cf. Figure 4a). The centers of these clusters have higher value of the  $x$  coordinate than the fault-free experimental run #1. This is in accordance with the model (3). A bearing surface damage is represented by repetitive excitations of bearing’s eigenmode(s), which in essence increases the bandwidth of the produced vibrations.

Although, the runs with bearing faults show some decrease of the  $C_t$  value, this effect is mostly visible for cases of pure gear faults (#2 and #3) (cf. Figure 4b) and the experimental runs #6 and #8. It can be noticed that unlike the bearing faults, the gear faults retain the spread in the frequency domain to some extent. Namely, the interval of the  $C_f$  values for the experimental runs #2 and #3 coincides with the interval of the fault-free run. The decrease of the  $C_t$  value can be mainly attributed to the increase of the amplitude  $A_m$  of the spectral components connected with the meshing gears, according to the model (1). Consequently, the time domain signal becomes dominated by a strong modulation, which results in decrease of the value of  $C_t$ . The same observation can be performed for the experimental runs #6 and #8 (cf. Figure 4a). Although these two runs include bearing faults, the lower wavelet time entropy is a result of the presence of shaft imbalance which introduces an additional strong periodic pattern in the signal, which is absent in the fault-free runs.

The distribution of the same wavelet entropies for low load is shown in Figure 5. As in the case of high load, the fault-free runs tend to locate in the upper left corner of the plots, thus having high values for  $C_t$  and low values for  $C_f$ . Although, generally the same observations made for the case of high load apply here too, the most significant difference is in the spread of values of  $C_t$  ( $y$ -axis).

For both mixed bearing (cf. Figure 5a) and pure gear faults (cf. Figure 5b), the fault clusters are spread over a narrower interval of  $C_t$  than in the case of high load. This is a direct consequence of the influence of the applied lower load. The amplitudes of the vibrational patterns produced by a particular fault are correspondingly lower, and hence insufficient for a significant change in the time behavior of the wavelet coefficients. This effect is expressed in the cases of pure gear faults (cf. Figure 5b), since the values  $A_m$  in (1) are directly related to the applied load. If we compare these results with those from the runs performed under high load (cf. Figure 4b), we can see that values of  $C_t$  are spread in the interval [4.6–5.2] for low load, whereas for the same faults the values of  $C_t$  are spread in the interval [3.8–4.8] for the high load cases. Consequently, some fault clusters might intersect with the fault-free cluster in the cases of lower load, like the experimental runs #3 and #5. Despite such overlaps, the centers of the fault clusters are sufficiently far apart for a rough decision about the presence of a fault.

**Combining SK with wavelet coefficient entropy** The results of each method have shown that in the majority of the cases the presence of fault can be detected without any knowledge of the operating conditions. However there were some cases in which the fault clusters intersect with the fault-free cluster and consequently there was a possibility of improper decision. By incorporating the SK values with the values of ICFs we expand the feature space. Such an extension subsequently contributes to better diagnostic resolution. The final feature space incorporating the three selected features is shown in Figure 6.

The ellipsoids in Figure 6, represent the dispersion in the feature space for the particular faults. In the case of low load (cf. Figure 6a), faults #2, #3 and #5 are grouped near the fault-free run #1. Despite the closeness, the fault-clusters are clearly distinguishable. This is most clearly visible in the cases of high load (cf. Figure 6b), where the fault-free cluster is completely isolated in the top right corner of the feature space. Furthermore, the intersection among the fault clusters are directly connected with the intersections of the faults which were present in each experimental run (cf. Table 1). Finally, we can conclude that based on the proposed feature set a proper fault detection can be performed without a precise knowledge of the current operating conditions.

## 5. CONCLUSION

In this paper we present a method for detecting mechanical faults in rotational machines subjected to variable operating conditions (load and speed). The fault detection process is based upon features extracted from the distribution of the wavelet packet coefficients in both time and frequency domain as well as the highest value of the

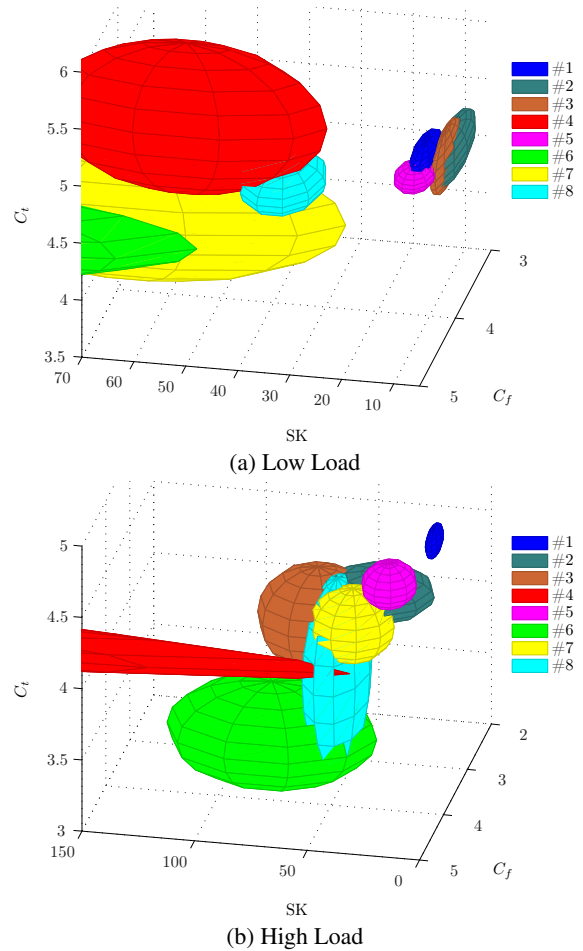


Figure 6: Ellipsoids representing the portion of the feature space occupied by a particular fault cluster. The radii of the ellipsoids represent the  $3\sigma$  spread of particular feature along the corresponding feature axis.

spectral kurtosis. Using these features a variety of mechanical faults were successfully detected using vibration data acquired from a two-stage gearbox.

The underlying approach has several characteristics that makes it suitable candidate for the task of fault detection. Firstly, both wavelet transform and spectral kurtosis methods can be seamlessly applied for analysis of non-stationary signals. This characteristic makes these methods suitable for analysis of vibration signals produced by a rotational machines operating under variable conditions. Secondly, the values of the extracted features are independent of the current rotational speed. This in essence removes the need of accurate rotational speed measurements. Finally, both methods can be implemented by using computationally efficient algorithms, the short-time Fourier transform for the spectral kurtosis and fast wavelet transform for the wavelet packet decomposition.

The extracted features have shown to be sensitive to the two major changes in the vibration signals that occur as a result of mechanical fault. Firstly, the Information Cost Function representing the order of the wavelet co-

efficient in the time domain is capable to detect the presence of specific patterns in the signal's waveform. Secondly, the presence of new spectral components affects the value of the information cost function representing the energy distribution in frequency domain. Furthermore, the spectral kurtosis serves as an indicator for the frequency band in which the previous two characteristics are mostly expressed. All these characteristics make the selected feature space an appropriate choice for the process of fault detection under variable operating conditions.

The results also show that the selected features tend to group in distinctive clusters that correspond to a particular fault. Such a behavior represents a prospect of upgrading the present fault detection process with a fault isolation task that will be based upon the location of the current feature values with regard to a previously determined clusters of faults.

### ACKNOWLEDGEMENTS

The research of the first author was supported by Ad futura Programme of the Slovenian Human Resources and Scholarship Fund. We also like to acknowledge the support of the Slovenian Research Agency through Research Programme P2-0001.

### REFERENCES

- Antoni, J., & Randall, R. (2006). The spectral kurtosis: a useful tool for characterising non-stationary signals. *Mechanical Systems and Signal Processing*, 20, 282-307.
- Bartelmus, W., & Zimroz, R. (2009). A new feature for monitoring the condition of gearboxes in non-stationary operating conditions. *Mechanical Systems and Signal Processing*, 23(5), 1528-1534.
- Baydar, N., & Ball, A. (2000). Detection of Gear deterioration under varying load conditions using the Instantaneous Power Spectrum. *Mechanical Systems and Signal Processing*, 14(6), 907-921.
- Blanco, S., Figliola, A., Quiroga, R. Q., Rosso, O. A., & Serrano, E. (1998). Time-frequency analysis of electroencephalogram series. III. Wavelet packets and information cost function. *Phys. Rev. E*, 57(1), 932-940.
- Burrus, C. S., Gopinath, R. A., & Guo, H. (1994). *Introduction to Wavelets and Wavelet Transforms: A Primer*. New Jersey: Prentice Hall.
- Dwyer, R. (1983). Detection of non-Gaussian signals by frequency domain Kurtosis estimation. *Acoustics, Speech, and Signal Processing, IEEE International Conference on ICASSP*, 8, 607-610.
- Feng, Y., & Schlindwein, F. S. (2009). Normalized wavelet packets quantifiers for condition monitoring. *Mechanical Systems and Signal Processing*, 23(3), 712-723.
- Figliola, A., & Serrano, E. (1997). Analysis of Physiological Time Series Using Wavelet Transforms. *IEEE Engineering in Medicine and Biology*, 16(3), 74-79.
- Howard, I., Jia, S., & Wang, J. (2001). The dynamic modelling of a spur gear in mesh including friction and crack. *Mechanical Systems and Signal Processing*, 15, 831-853.
- Kuang, J.-H., & Li, A.-D. (2003). Theoretical aspects of torque responses in spur gearing due to mesh stiffness variation. *Mechanical Systems and Signal Processing*, 17, 255-271.
- Mallat, S. (1999). *A wavelet tour of signal processing, Second edition*. San Diego: Academic Press.
- Parker, B. E., Ware, H. A., Wipf, D. P., Tompkins, W. R., Clark, B. R., & Larson, E. C. (2000). Fault Diagnosis using Statistical change detection in the Bispectral Domains. *Mechanical Systems and Signal Processing*, 14(4), 561-570.
- Percival, D. B., & Walden, A. T. (2000). *Wavelet Methods for Time Series Analysis*. Cambridge: Cambridge University Press.
- PHM. (2009). *Prognostics and Health Management Society 2009 Data Challenge*. <http://www.phmsociety.org/competition/09>.
- Priestley, M., & Gabr, M. (1993). Multivariate Analysis: Future Directions. In C. Rao (Ed.), (Vol. 5, pp. 295-317). Amsterdam: North-Holland, Elsevier.
- Randall, R. B., Antoni, J., & Chobsaard, S. (2001). The relationship between spectral correlation and envelope analysis in the diagnostics of bearing faults and other cyclostationary machine signals. *Mechanical Systems and Signal Processing*, 15, 945-962.
- Rosso, O. A., Blanco, S., Yordanova, J., Kolev, V., Figliola, A., Schürmann, M., et al. (2001). Wavelet entropy: a new tool for analysis of short duration brain electrical signals. *Journal of Neuroscience Methods*, 105(1), 65-75.
- Spanos, P. D., & Failla, G. (2004). Evolutionary Spectra Estimation Using Wavelets. *Journal of Engineering Mechanics*, 130(8), 952-960.
- Stander, C., & Heyns, P. (2005). Instantaneous angular speed monitoring of gearboxes under non-cyclic stationary load conditions. *Mechanical Systems and Signal Processing*, 19(4), 817-835.
- Wang, W. (2001). Early Detection of gear tooth cracking using the resonance demodulation technique. *Mechanical Systems and Signal Processing*, 15, 887-903.
- Zhan, Y., Makis, V., & Jardine, A. K. (2006). Adaptive state detection of gearboxes under varying load conditions based on parametric modelling. *Mechanical Systems and Signal Processing*, 20(1), 188-221.
- Zunino, L., Pérez, D., Garavaglia, M., & Rosso, O. (2007). Wavelet entropy of stochastic processes. *Physica A: Statistical Mechanics and its Applications*, 379(2), 503-512.